



Universiteit
Leiden
The Netherlands

OX40L Inhibition suppresses KLH-driven immune responses in healthy volunteers: a randomized controlled trial demonstrating proof-of-pharmacology for KY1005

Saghari, M.; Gal, P.; Gilbert, S.; Yatemán, M.; Porter-Brown, B.; Brennan, N.; ... ; Rissmann, R.

Citation

Saghari, M., Gal, P., Gilbert, S., Yatemán, M., Porter-Brown, B., Brennan, N., ... Rissmann, R. (2022). OX40L Inhibition suppresses KLH-driven immune responses in healthy volunteers: a randomized controlled trial demonstrating proof-of-pharmacology for KY1005. *Clinical Pharmacology & Therapeutics*, 111(5), 1121-1132. doi:10.1002/cpt.2539

Version: Publisher's Version
License: [Creative Commons CC BY-NC 4.0 license](https://creativecommons.org/licenses/by-nc/4.0/)
Downloaded from: <https://hdl.handle.net/1887/3483886>

Note: To cite this publication please use the final published version (if applicable).

OX40L Inhibition Suppresses KLH-driven Immune Responses in Healthy Volunteers: A Randomized Controlled Trial Demonstrating Proof-of-Pharmacology for KY1005

Mahdi Saghari^{1,2}, Pim Gal^{1,2}, Sally Gilbert³, Martin Yateman³, Ben Porter-Brown³, Nuala Brennan³, Sonia Quarantino³, Rosamund Wilson³, Hendrika W. Grievink^{1,4}, Erica S. Klaassen¹, Kirsten R. Bergmann¹, Jacobus Burggraaf^{1,2,4}, Martijn B. A. van Doorn^{1,5}, John Powell³, Matthijs Moerland^{1,2} and Robert Rissmann^{1,2,4,*}

The safety, tolerability, immunogenicity, and pharmacokinetic (PK) profile of an anti-OX40L monoclonal antibody (KY1005, currently amltelimab) were evaluated. Pharmacodynamic (PD) effects were explored using keyhole limpet hemocyanin (KLH) and tetanus toxoid (TT) immunizations. Sixty-four healthy male subjects (26.5 ± 6.0 years) were randomized to single doses of 0.006, 0.018, or 0.05 mg/kg, or multiple doses of 0.15, 0.45, 1.35, 4, or 12 mg/kg KY1005, or placebo (6:2). Serum KY1005 concentrations were measured. Antibody responses upon KLH and TT immunizations and skin response upon intradermal KLH administration were performed. PD data were analyzed using repeated measures analysis of covariances (ANCOVAs) and post hoc exposure-response modeling. No serious adverse events occurred and all adverse events were temporary and of mild or moderate severity. A nonlinear increase in mean serum KY1005 concentrations was observed (median time to maximum concentration (T_{max}) ~ 4 hours, geometric mean terminal half-life ($t_{1/2}$) ~ 24 days). Cutaneous blood perfusion (estimated difference (ED) -13.4 arbitrary unit (AU), 95% confidence interval (CI) -23.0 AU to -3.8 AU) and erythema quantified as average redness (ED -0.23 AU, 95% CI -0.35 AU to -0.11 AU) decreased after KY1005 treatment at doses of 0.45 mg/kg and above. Exposure-response analysis displayed a statistically significant treatment effect on anti-KLH antibody titers (IgG maximum effect (E_{max}) -0.58 AU, 95% CI -1.10 AU to -0.06 AU) and skin response (erythema E_{max} -0.20 AU, 95% CI -0.29 AU to -0.11 AU). Administration of KY1005 demonstrated an acceptable safety and tolerability profile and PK analyses displayed a nonlinear profile of KY1005. Despite the observed variability, skin challenge response after KY1005 treatment indicated pharmacological activity of KY1005. Therefore, KY1005 shows potential as a novel pharmacological treatment in immune-mediated disorders.

Study Highlights

WHAT IS THE CURRENT KNOWLEDGE ON THE TOPIC?

✓ Activation of the OX40-OX40L pathway possibly contributes to resistance of T lymphocytes to regulatory signals and, therefore, OX40-OX40L signaling may be a target for the treatment of auto-immune diseases.

WHAT QUESTION DID THIS STUDY ADDRESS?

✓ The aim of this first-in-human study was to evaluate the safety and tolerability, immunogenicity, and pharmacokinetic profile of KY1005 (anti-OX40L monoclonal antibody) in healthy volunteers. Pharmacodynamic effects of KY1005 were explored using a keyhole limpet hemocyanin challenge model.

WHAT DOES THIS STUDY ADD TO OUR KNOWLEDGE?

✓ Proof-of-pharmacology for KY1005 was demonstrated as this study shows that interference with OX40-OX40L signaling via KY1005 modified the neoantigen immune response.

HOW MIGHT THIS CHANGE CLINICAL PHARMACOLOGY OR TRANSLATIONAL SCIENCE?

✓ The observed immunomodulatory properties of KY1005 support the development of the drug, and other OX40-OX40L pathway targeting compounds, for the treatment of immune-mediated disorders.

¹Centre for Human Drug Research, Leiden, The Netherlands; ²Leiden University Medical Centre, Leiden, The Netherlands; ³Kymab Ltd., Cambridge, UK; ⁴Leiden Academic Centre for Drug Research, Leiden, The Netherlands; ⁵Department of Dermatology, Erasmus Medical Centre, Rotterdam, The Netherlands. *Correspondence: Robert Rissmann (rissmann@chdr.nl)

Trial identifiers: EudraCT number: 2016-004839-20, ClinicalTrials.gov Identifier: NCT03161288.

Received October 13, 2021; accepted January 20, 2022. doi:10.1002/cpt.2539

The significance of the T cell costimulatory molecule OX40 and its ligand OX40L in immunoregulation is increasing, especially as therapeutic targets. OX40 is predominantly expressed on activated memory and regulatory cluster of differentiation 4 (CD4+) T cells and in lower levels on activated CD8+ T cells,¹ natural killer cells^{2,3} and neutrophils.⁴ OX40 agonism has been shown to result in an increase of the antigen-specific T cell pool^{5,6} and prolonged activation.⁷ Similar to OX40, the expression of OX40L is upregulated after antigen presentation on various antigen-presenting cells such as B cells,⁸ dendritic cells,⁹ macrophages¹⁰ and specific cell types outside the immune system.^{11–14} Activation of this costimulatory OX40-OX40L pathway may contribute to resistance of T lymphocytes to regulatory signals.¹⁵

OX40-OX40L signaling may be a target for the treatment of auto-immune diseases.^{16–21} Several animal models confirmed that OX40L is involved in diabetes,²² colitis,²³ rheumatoid arthritis,²⁴ uveitis,²⁵ and multiple sclerosis.^{26,27} In human studies, OX40 inhibition using an anti-OX40 monoclonal antibody has been shown to improve the Eczema Area and Severity Index (EASI) score in patients with atopic dermatitis with up to 56% reduction from baseline EASI score compared with 38% reduction in placebo-treated subjects.²⁰ Another study showed that although OX40L inhibition with an anti-OX40L monoclonal antibody in patients with mild allergic asthma had no effect on airway hyperresponsiveness or allergen-induced airway responses, total serum immunoglobulin E (IgE) decreased 16.5% from baseline compared with a 14% increase in placebo-treated subjects and sputum eosinophils decreased 75% from baseline compared with a 14% decrease in placebo-treated subjects.²⁸ Blockade of the OX40-OX40L pathway seems a scientifically plausible approach to modulate persistent inflammation caused by autoreactive memory T effector cell populations. This blockade may possibly also induce or restore immune tolerance to autoantigens (e.g., in autoimmune disease) or alloantigens (e.g., following transplants).

KY1005 (also known as SAR445229 and currently as amlitelimab) is a novel nondepleting IgG4 human anti-OX40L monoclonal antibody that binds OX40L and thereby prevents persistent inflammation by blocking the interaction with OX40. *In vitro*, KY1005 inhibited interleukin 2 (IL-2), IL-13, and tumor necrosis factor α release in human mixed lymphocyte reaction (MLR) tests (**Supplementary Materials and Methods S1**). *In vivo* studies in rhesus monkeys with acute graft-versus-host disease showed prolonged median survival time (MST) > 100 days when KY1005 was co-administered with sirolimus compared with KY1005 monotherapy (MST 19.5 days), sirolimus monotherapy (MST 14 days), or no prophylaxis (MST 8 days).²⁹ The synergistic effect of KY1005/sirolimus was possibly induced by sustained T regulatory cell reconstitution as well as suppression of T effector activity. Based on these experiments, KY1005 could be a treatment modality to inhibit the activation of the immune system as a result of high OX40-OX40L expression and consequently restore the homeostasis between pro-inflammatory T effector and anti-inflammatory T regulatory cells in immune-mediated diseases.

The aim of this first-in-human study was to evaluate the safety and tolerability, immunogenicity, and pharmacokinetic (PK) profile of KY1005 in healthy volunteers. Intramuscular immunizations

with a neoantigen (keyhole limpet hemocyanin (KLH)) and a recall antigen (tetanus toxoid (TT)) were used to explore pharmacodynamic (PD) effects of KY1005, including measurements of serum anti-KLH and anti-TT antibody titers and objective quantification of skin challenge response following an intradermal KLH administration.

MATERIALS AND METHODS

This was a phase I, randomized, placebo-controlled, double-blind, single ascending dose (SAD) and multiple ascending dose (MAD) study in 64 healthy volunteers performed at the Centre for Human Drug Research (CHDR), Leiden, The Netherlands. The Declaration of Helsinki was the principle for trial execution. The independent Medical Ethics Committee “Medisch Ethische Toetsingscommissie van de Stichting Beoordeling Ethiek Biomedisch Onderzoek” (Assen, The Netherlands) approved the study prior to any clinical study activity. All subjects provided written informed consent before participation. The trial was registered on ClinicalTrials.gov (NCT03161288).

Subjects

Main inclusion criteria were male gender, 18–45 years of age, with a body mass index between 18 and 30 kg/m², and previous immunization with TT more than 6 months prior to screening and no known previous exposure to KLH. Health status was verified by recording a detailed medical history, a complete physical examination, vital signs, a 12-lead electrocardiogram (ECG), and laboratory testing (including hepatic and renal panels, complete blood count, virology, and urinalysis). Subjects were excluded in case of any disease associated with immune system impairment, or use of prescription medication within 2 weeks prior to enrollment.

Dose selection and regimen

The starting dose of 0.006 mg/kg KY1005 was based on a minimal anticipated biological effect level (MABEL) principle using *in vitro* data obtained in human MLR experiments. The maximum dose of 12 mg/kg KY1005 was based on the maximal effects observed in these experiments and predicted exposure equivalent to that at which maximum *in vivo* inhibition of the IgG response to KLH immunization occurred in monkeys. Detailed information on dose selection can be found in **Supplementary Materials and Methods S1**. The interval of 4 weeks between the loading dose and 2 maintenance doses was based on scaling of the KY1005 terminal half-life ($t_{1/2}$) of 23 ± 1 day observed in cynomolgus monkeys. Threefold dose increments between cohorts were based on a 30-fold difference in concentration between the lowest effects and maximal effects observed in the MLR experiments, a modest slope of the dose response and theoretical risks related to OX40L blocking.

Study design and treatments

An overview of the study design is shown in **Figure S1**. Subjects were enrolled into eight cohorts. In each cohort, subjects were randomized to either 30 minutes of intravenous administration of KY1005 or placebo (6:2). Two subjects per cohort started as a sentinel group and if no safety issues arose within 48 hours after dosing, the remaining 6 subjects were dosed. The first 3 cohorts received single doses of 0.006, 0.018, or 0.05 mg/kg KY1005, respectively. The 5 subsequent cohorts received multiple doses starting with an initial loading dose of 0.15, 0.45, 1.35, 4, or 12 mg/kg KY1005, respectively, followed by 2 maintenance doses of 50% of the loading dose, administered at 4 and 8 weeks after the initial administration. Intramuscular KLH and TT immunizations were performed in the deltoid muscles 1 week after the last (third) KY1005/placebo dose in the MAD cohorts. KLH was administered in a formulation of 0.1 mg of subunit KLH (Immucothel, biosyn, Fellbach, Germany) adsorbed in 0.9 mg aluminium hydroxide (Alhydrogel, Brenntag Biosector A/S, Frederikssund, Denmark) into 0.5 mL NaCl 0.9%, as described

previously.³⁰ TT was administered in the marketed formulation of ≥ 40 IU TT (Bilthoven Biologicals, Bilthoven, The Netherlands) in 0.5 mL NaCl 0.9%.^{31,32} Twenty-one days after intramuscular KLH administration, all subjects received an intradermal KLH administration in the left ventral forearm and placebo administration in the right ventral forearm. The formulation of 0.001 mg subunit KLH in 0.1 mL NaCl 0.9% used for intradermal administration was based on a previously conducted trial.³⁰ The interval of 21 days between intramuscular KLH immunization and intradermal KLH administration and the interval of 48 hours between baseline and follow-up skin challenge assessment has been used in previous other studies.^{30,31,33–36} Prior to and 2 days after the intradermal KLH administration, the skin challenge response was quantified.

Safety and tolerability

Safety and tolerability were monitored by physical examination, assessment of vital signs, laboratory parameters (i.e., full blood count, biochemistry, and urinalysis) and ECG data from 12-lead and 24-hour Holter ECGs at regular intervals. Subjects were monitored continuously for adverse events (AEs).

KY1005 pharmacokinetics and immunogenicity

Serum concentrations of KY1005 for PK profiling and serum concentrations of antidrug antibodies (ADAs) were measured by Eurofins Pharma Bioanalysis Services UK Ltd. (Abingdon, UK) using validated bioanalytical assay methods. The PK samples were analyzed using a luminescent enzyme-linked immunosorbent assay with a lower limit of quantification (LLOQ) of 9.77 ng/mL. ADAs were measured using an electrochemoluminescence solid-phase extraction with acid dissociation method. In both ADA screening and confirmatory formats, the assay tolerated up to 100 μ g/mL KY1005 at positive control anti-KY1005 antibody concentrations of 100 and 250 ng/mL.

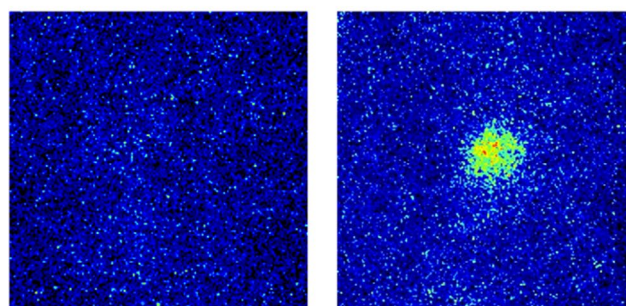
OX40 and OX40L expression

OX40 and OX40L expression was measured by CHDR (Leiden, The Netherlands) on cell subsets of whole blood samples using flow cytometry. Red blood cell lysis was performed on heparinized whole blood using RBC lysis buffer (Thermo Fisher, Waltham, MA, USA). Leukocytes were stained with fluorochrome labelled antibodies at 4°C for 30 minutes, see **Table S1** for a complete list. After staining, the cells were washed with PBS (Thermo Fisher). Samples were measured on a MACSQuant 10 analyzer, and analyzed using MACSQuantify software (both Miltenyi Biotec, Bergisch-Gladbach, Germany). See **Figure S2** for the gating strategy. OX40 expression was assessed in CD4+ and CD8+ T cells, regulatory T cells and Th17 cells and OX40L expression was assessed in CD19+ and CD14+ monocytes in all cohorts. In addition, expression of OX40 and OX40L in CD4+ and CD8+ effector memory and central memory cells was assessed in cohorts 4–8.

Humoral immunity to KLH and TT

The humoral response to intramuscular KLH and TT immunization was measured by anti-KLH and anti-TT IgM and IgG blood serum titers 21 days after immunization. Serum samples were assessed by quantitative enzyme-linked immunosorbent assay for anti-KLH and anti-TT IgM and IgG levels, as previously described.³⁰ In KLH-immunized subject blood samples, mean optical density of baseline samples was set to 1.00 and ratios relative to baseline were calculated for all subsequent samples. The LLOQ and the upper limit of quantification (ULOQ) for anti-KLH IgM and IgG were a baseline corrected optical density of 0.060 and 3.900, respectively. The LLOQ and ULOQ for anti-TT IgM were 10.0 and 100 IU/mL, respectively, and the LLOQ and ULOQ for anti-TT IgG were 0.100 and 5.00 IU/mL, respectively.

LSCI basal flow



Multispectral imaging average redness

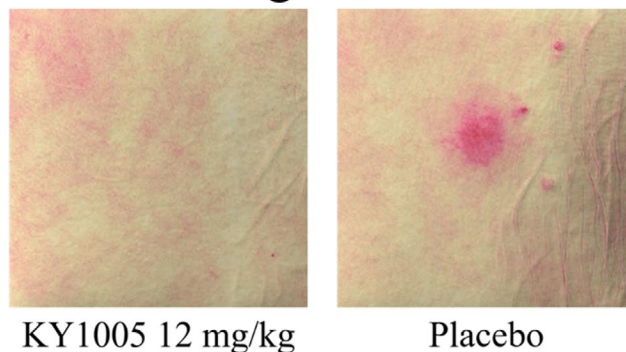


Figure 1 Illustrations of LSCI basal flow and erythema assessed as average redness with multispectral imaging. Images were taken at intradermal KLH injection site 2 days after intradermal KLH administration of a subject treated with an initial KY1005 12 mg/kg dose (left images) and a subject that received placebo (right images). KLH, keyhole limpet hemocyanin; LSCI, laser speckle contrast imaging.

Cutaneous blood perfusion

Cutaneous blood perfusion quantification was performed with laser speckle contrast imaging (LSCI; PeriCam PSI System, Perimed AB, Järfälla, Sweden), as previously described.³⁰ In short, assessments were performed in a temperature-controlled room (22°C) after acclimatization of the subjects. LSCI recordings of the target area on the left and right ventral forearms were captured with the use of dedicated software (PimSoft, Perimed AB). Circular regions of interest at the intradermal injection sites were defined and cutaneous blood perfusion (indicated as basal flow) was quantitatively assessed and expressed in arbitrary units (AUs). The homogeneity of cutaneous blood perfusion in the region of interest (indicated as flare), expressed as values that are +1 standard deviation (SD) from the mean basal flow within the region, was also quantitatively assessed and expressed in AUs. Illustrations of cutaneous blood perfusion measured with LSCI are depicted in **Figure 1**.

Erythema

Erythema quantification was performed with multispectral imaging (Antera 3D; Miravex, Dublin, Ireland), as previously described.³⁰ In short, the camera was placed on the target area on the ventral forearms and images were captured using dedicated software (Antera 3D software, Miravex). Circular regions of interest at the intradermal injection sites were defined and erythema was quantified using the average redness and

CIELab a* Antera 3D software modalities expressed as AUs. The average redness modality displays the distribution of redness using an internal software algorithm and the CIELab a* value, which is part of the CIELab color space, expresses color as a numerical value on a green–red color scale.³⁷ Illustrations of erythema measured with multispectral imaging are depicted in **Figure 1**.

Statistics

Detailed statistical procedures used in the current study are provided in the **Supplementary Materials and Methods S1**. Subjects were randomized to KY1005 or placebo in a 3:1 ratio. Demographic and baseline variables were summarized by treatment. For safety and tolerability end points, summary statistics for observed values were calculated for all continuous parameters. For every KY1005 dose, the peak serum concentration (C_{max}), $t_{1/2}$, area under the curve from zero to the last measurable concentration (AUC_{0-last}) and clearance (CL) were reported as mean (coefficient of variation percentage (CV%)) and the time at which C_{max} is observed (T_{max}) was reported as median (range). PD end points measured at multiple timepoints post baseline were analyzed with a mixed effect repeated measures model. End points with one postdose measurement were analyzed with an analysis of covariance (ANCOVA) model. Skin challenge end points were analyzed with ANCOVA with the change from the saline-injected control (right forearm) added as covariate. The general treatment effect and specific contrasts were reported with the estimated difference (ED), 95% confidence interval (CI), and P value, and graphically as ED, 95% CI, and P value or mean change from baseline, SD, and P value. Negative change from baseline values for skin challenge end points were possible due to measurement variability and the dynamic nature of the measurements. Nonlinear mixed effects analysis of the exposure-response relationship was performed for anti-KLH and anti-TT antibody titers and skin challenge end points.

RESULTS

Baseline characteristics

The study was conducted between May 2017 and March 2018. Twenty-four (24) subjects were enrolled in the SAD part and 40 subjects in the MAD part of the study. Four subjects did not complete the study: one subject was withdrawn due to a suspected hypersensitivity reaction consisting of pruritus, swelling of the palate and gums, and slurred speech lasting ~ 2 hours after the first dose, 3 subjects withdrew consent for reasons unrelated to the study treatment. Baseline characteristics of all treatment groups are presented in **Table 1**.

Safety and tolerability

No serious AEs occurred during the study. One subject in the MAD part of the study (12 mg/kg cohort) did not receive the second and third KY1005 doses due to a possible hypersensitivity reaction (mild palatal pruritus and swelling and slurred speech) after the first dose. No medication was administered based on the mild nature of the AEs and all symptoms resolved within 2 hours. Additional blood chemistry and hematology, including complement activation markers and tryptase, were all within normal ranges. No other AE-related discontinuations occurred during the study. The most frequently occurring treatment emergent AE was headache (**Tables S2, S3**). All treatment emergent AEs were of mild ($n = 190$) or moderate severity ($n = 16$) and self-resolving without sequelae. Treatment did not result in any clinically significant changes in any safety laboratory parameters, physical

examination, vital signs measures, 12-lead ECG recordings, and Holter ECG recordings (data not shown).

KY1005 pharmacokinetics and immunogenicity

A dose-dependent increase in mean serum concentrations of KY1005 was observed after single administrations (cohorts 1–3) and after multiple administrations (cohorts 4–8; **Figure 2**). KY1005 reached $T_{max} \sim 4$ hours after the start of infusion (median across cohorts from 0.5–24 hours) and had a $t_{1/2}$ of ~ 24.3 days (mean across cohorts from 7.1 to 43.1 days with CV% of 15.5%–51.8%; **Table 2**). Overall, single or multiple doses of KY1005 as measured by noncompartmental PK analysis appeared to be non-linear (**Table 2**). KY1005 clearance remained relatively stable at concentrations > 2 mg/mL approximately (data not shown).

The number of subjects with ADAs increased with increasing KY1005 dose in cohorts 1–3 (2, 2, and 5 subjects, respectively). In cohorts 4–8, however, the largest number of subjects positive for ADAs (4 subjects) was observed at the lowest dose regime (0.15 mg/kg KY1005 cohort), with no subjects developing detectable ADAs at the highest dose (12 mg/kg KY1005 cohort). There was no correlation between ADAs and any of the PK parameters, including CL (data not shown).

OX40 and OX40L expression

No consistent OX40 and OX40L expression profile trends were observed across the groups, although some P values < 0.05 compared with placebo were noted (**Table S4**). The differences compared with placebo in OX40 and OX40L expression on a variety of immune cells did not induce any clinically relevant observations.

Humoral immunity to KLH and TT

Although no statistical significance was reached, KY1005 treatment seemed to suppress the anti-KLH IgM and IgG antibody response after intramuscular KLH immunization (**Figure 3a,b**). KY1005 appeared to have a PD effect from doses of 0.45 mg/kg and above based on the anti-KLH IgG response. The ED between KY1005 and placebo-treated subjects was maximally –32.4% (95% CI –54.7%–0.9%, $P = 0.06$) observed for anti-KLH IgG at the highest KY1005 dose of 12 mg/kg (**Table 3**). No consistent effect of KY1005 on anti-TT IgM and IgG antibodies was observed (**Table 3, Figure 3c,d**).

Exposure-response modeling of humoral immunity to KLH and TT

Given the small sample size, post hoc KY1005 exposure-response modeling was performed. This analysis showed a modest treatment effect of KY1005 (Akaike's Information Criteria maximum effect ($AIC_{Emax\ model} < AIC_{no-effect\ model}$) on anti-KLH IgM ($E_{max} -0.22$ AU, 95% CI –0.46 AU to 0.02 AU) and IgG antibody titers ($E_{max} -0.58$ AU, 95% CI –1.10 AU to –0.06 AU), whereas no exposure-response was observed on anti-TT IgM and anti-TT IgG antibody titers (**Figure 4a–d**), based on the exposure-response model. The 50% of the maximal effect (EC_{50}) could not be reliably determined for any of the variables, likely due to the high variability of the measurements as well as the small sample size.

Table 1 Baseline characteristics

	SAD						MAD					
	KY1005			Placebo			KY1005			Placebo		
	0.006 mg/kg	0.018 mg/kg	0.05 mg/kg	NA	NA	NA	0.15 mg/kg	0.45 mg/kg	1.35 mg/kg	4 mg/kg	12 mg/kg	NA
Loading dose												
Maintenance doses	NA	NA	NA	NA	NA	NA	0.075 mg/kg	0.225 mg/kg	0.675 mg/kg	2 mg/kg	6 mg/kg	NA
	N = 6	N = 6	N = 6	N = 6	N = 6	N = 6	N = 6	N = 6	N = 6	N = 6	N = 6	N = 10
DEMOGRAPHICS												
Age, years	24.3 (4.5)	23.8 (1.5)	25.3 (3.7)	26.2 (7.1)	28.0 (9.2)	23.3 (3.9)	24.8 (3.9)	24.7 (4.1)	34.2 (6.3)	28.5 (5.6)		
BMI, kg/m ²	22.9 (1.3)	21.7 (1.5)	23.5 (2.8)	23.5 (2.2)	22.9 (2.2)	23.1 (3.1)	22.8 (2.3)	23.1 (1.8)	24.9 (3.0)	24.5 (3.1)		
VITAL SIGNS												
Systolic blood pressure, mmHg	119 (8)	115 (11)	126 (11)	121 (16)	118 (3)	120 (11)	123 (13)	118 (11)	127 (7)	122 (9)		
Diastolic blood pressure, mmHg	72 (5)	68 (8)	77 (6)	68 (12)	72 (9)	75 (10)	68 (9)	70 (13)	78 (8)	72 (13)		
Heart rate, bpm	57 (13)	59 (7)	68 (11)	63 (17)	57 (8)	59 (8)	63 (14)	59 (10)	67 (9)	61 (8)		
Temperature, °C	36.7 (0.3)	36.9 (0.1)	36.8 (0.6)	36.7 (0.3)	36.4 (0.3)	36.9 (0.2)	36.5 (0.4)	36.5 (0.2)	36.6 (0.5)	36.6 (0.2)		
LABORATORY TESTS												
Leucocytes, *10 ⁹ /L	6.61 (1.05)	6.10 (1.58)	5.89 (1.06)	5.94 (0.96)	5.21 (1.16)	5.66 (0.86)	6.75 (1.52)	6.59 (1.59)	6.57 (1.19)	6.05 (2.42)		
Thrombocytes, *10 ⁹ /L	244.5 (26.4)	279.2 (68.1)	267.3 (43.0)	215.3 (40.1)	254.4 (69.8)	270.7 (53.8)	229.2 (29.6)	216.3 (53.3)	269.6 (65.7)	253.2 (53.7)		
ALT, IU/L	18.0 (5.8)	13.7 (4.2)	16.5 (3.6)	16.2 (7.1)	23.2 (14.1)	20.2 (11.7)	31.3 (20.1)	24.8 (19.0)	30.3 (11.7)	22.2 (7.0)		
AST, IU/L	23.2 (9.1)	20.7 (5.3)	19.2 (3.6)	18.2 (5.1)	22.7 (6.0)	24.0 (4.8)	28.5 (9.4)	25.3 (8.7)	27.0 (8.7)	21.2 (5.8)		

Parameters are shown as mean (SD).

ALT, alanine aminotransferase; AST, aspartate aminotransferase; BMI, body mass index; MAD, multiple ascending dose; NA, not applicable; SAD, single ascending dose.

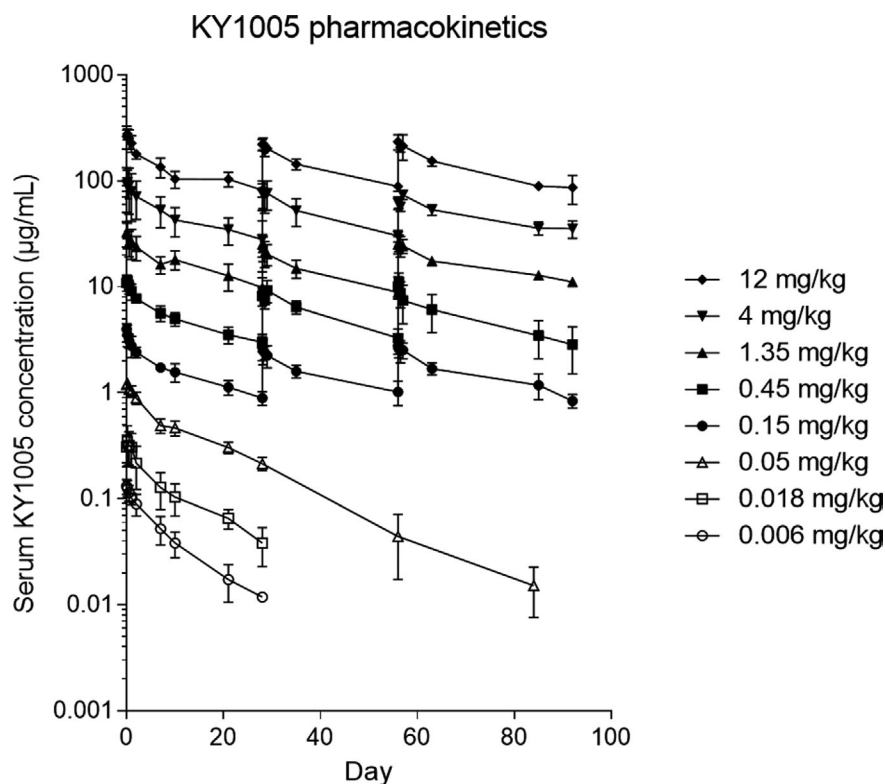


Figure 2 KY1005 serum concentrations ($\mu\text{g/mL}$). Data displayed on log₁₀ scale as mean (SD).

Cutaneous blood perfusion

Overall, KY1005 reduced the intradermal KLH-driven increase in cutaneous blood perfusion quantified by LSCI basal flow and flare (Table 3, Figure 3e,f). Although a clear dose dependence was absent, pharmacological KY1005 effects on LSCI basal flow and flare based on suppression of skin challenge response were observed at intermediate dose levels of 0.45 mg/kg (ED -13.4 AU, 95% CI -23.0 AU to -3.8 AU, $P < 0.01$ and ED -7.5 AU, 95% CI -13.2 AU to -1.8 AU, $P < 0.05$, respectively), 4 mg/kg (ED -11.0 AU, 95% CI -19.8 AU to -2.3 AU, $P < 0.05$ and ED -5.8 AU, 95% CI -10.8 AU to -0.9 AU, $P < 0.05$, respectively), and 12 mg/kg (ED -5.9 AU, 95% CI -14.4 AU to 2.5 AU, $P = 0.16$ and ED -3.1 AU, 95% CI -7.9 AU to -1.8 AU, $P = 0.21$, respectively; Figure 3e,f). All groups showed a reduced cutaneous blood perfusion response compared with placebo.

Erythema

KY1005 treatment also reduced erythema quantified by multispectral imaging as average redness and as CIELab a^* (Table 3, Figure 3g,h). Similar to the observations with LSCI multispectral imaging, average redness and CIELab a^* were decreased in the groups that received KY1005 as initial dose of 0.45 mg/kg (ED -0.20 AU, 95% CI -0.32 AU to -0.07 AU, $P < 0.01$ and ED -2.1 AU, 95% CI -3.5 AU to -0.8 AU, $P < 0.01$, respectively), 4 mg/kg (ED -0.17 AU, 95% CI -0.29 AU to -0.05 AU, $P < 0.01$ and ED -2.0 AU, 95% CI -3.4 AU to -0.7 AU, $P < 0.01$, respectively), and 12 mg/kg (ED -0.23 AU, 95% CI -0.35 AU to

-0.11 AU, $P < 0.001$ and ED -2.6 AU, 95% CI -4.0 AU to -1.3 AU, $P < 0.001$, respectively) compared with placebo (Table 3, Figure 3g,h).

Exposure-response modeling of skin challenge end points

Exposure-response modeling showed a treatment effect of KY1005 ($\text{AIC}_{\text{Emax model}} < \text{AIC}_{\text{no-effect model}}$) on LSCI basal flow (E_{max} -7.09 AU, 95% CI -13.23 AU to -0.96 AU), LSCI flare (E_{max} -4.77 AU, 95% CI -8.06 AU to -1.48 AU), multispectral imaging average redness (E_{max} -0.20 AU, 95% CI -0.29 AU to -0.11 AU) and CIELab a^* (E_{max} -2.10 AU, 95% CI -3.05 AU to -1.15 AU; Figure 4e-h), based on the exposure-response model. The EC_{50} could not be reliably determined for any of the variables, likely due to the high variability of the measurements as well as the small sample size.

DISCUSSION

In this first-in-human study, we showed that KY1005 was safe and well-tolerated and we demonstrated proof-of-pharmacology for KY1005 as the drug suppressed the KLH-driven neoantigen immune response via OX40-OX40L signaling interference, despite the observed variability in the skin challenge response.

Importantly, KY1005 treatment in the current study had an unremarkable safety and tolerability profile. One hypersensitivity reaction was observed in this study in one subject in the 12 mg/kg group that was possibly related to KY1005. An allergy to KY1005 or any excipients was considered unlikely, because this

Table 2 Summary of pharmacokinetic parameters of KY1005 per dose level

Parameter	SAD						MAD									
	0.006 mg/kg (N = 6)	0.018 mg/kg (N = 6)	0.05 mg/kg (N = 6)	0.15 mg/kg (N = 6)	0.45 mg/kg (N = 6)	1.35 mg/kg (N = 6)	4 mg/kg (N = 6)	12 mg/kg (N = 6)	0.006 mg/kg (N = 6)	0.018 mg/kg (N = 6)	0.05 mg/kg (N = 6)	0.15 mg/kg (N = 6)	0.45 mg/kg (N = 6)	1.35 mg/kg (N = 6)	4 mg/kg (N = 6)	12 mg/kg (N = 6)
First KY1005 dose																
T _{max} , h	0.5 (0.5–4.0)	4.0 (0.5–12.0)	2.3 (0.5–4.0)	0.5 (0.5–4.0)	4.0 (0.5–12.0)	2.3 (0.5–24.0)	2.3 (0.5–4.5)	4.0 (0.5–24.0)	0.5 (0.5–4.0)	4.0 (0.5–12.0)	2.3 (0.5–24.0)	0.5 (0.5–4.0)	4.0 (0.5–12.0)	2.3 (0.5–24.0)	2.3 (0.5–4.5)	4.0 (0.5–24.0)
C _{max} , µg/mL	0.1 (16.2%)	0.4 (40.4%)	1.3 (6.7%)	4.0 (12.4%)	11.8 (10.3%)	34.8 (24.0%)	112.2 (33.8%)	289.7 (17.5%)	0.1 (16.2%)	0.4 (40.4%)	1.3 (6.7%)	4.0 (12.4%)	11.8 (10.3%)	34.8 (24.0%)	112.2 (33.8%)	289.7 (17.5%)
t _{1/2} , days	7.1 (33.3%)	13.4 (41.3%)	12.1 (18.6%)	20.8 (26.9%)	23.1 (26.2%)	23.2 (44.7%)	20.3 (17.9%)	22.7 (21.9%)	7.1 (33.3%)	13.4 (41.3%)	12.1 (18.6%)	20.8 (26.9%)	23.1 (26.2%)	23.2 (44.7%)	20.3 (17.9%)	22.7 (21.9%)
AUC _{0–last} , µg*day/mL	0.9 (33.9%)	3.1 (31.1%)	17.3 (15.4%)	43.0 (8.9%)	138.5 (11.5%)	453.3 (18.2%)	1263.7 (30.3%)	3337.7 (7.5%)	0.9 (33.9%)	3.1 (31.1%)	17.3 (15.4%)	43.0 (8.9%)	138.5 (11.5%)	453.3 (18.2%)	1263.7 (30.3%)	3337.7 (7.5%)
CL, mL/min	0.30 (33.2%)	0.27 (58.7%)	0.15 (15.5%)	0.11 (19.7%)	0.10 (19.5%)	0.10 (26.5%)	0.12 (25.8%)	0.12 (19.1%)	0.30 (33.2%)	0.27 (58.7%)	0.15 (15.5%)	0.11 (19.7%)	0.10 (19.5%)	0.10 (26.5%)	0.12 (25.8%)	0.12 (19.1%)
Second KY1005 dose																
T _{max} , h	-	-	-	2.5 (0.5–12.5)	24.0 (4.6–24.0)	2.5 (0.5–24.0)	12.5 (0.5–24.0)	4.6 (0.5–24.0)	-	-	-	2.5 (0.5–12.5)	24.0 (4.6–24.0)	2.5 (0.5–24.0)	12.5 (0.5–24.0)	4.6 (0.5–24.0)
C _{max} , µg/mL	-	-	-	2.9 (20.9%)	9.8 (21.3%)	26.1 (19.3%)	89.6 (31.1%)	229.9 (11.7%)	-	-	-	2.9 (20.9%)	9.8 (21.3%)	26.1 (19.3%)	89.6 (31.1%)	229.9 (11.7%)
t _{1/2} , days	-	-	-	27.0 (51.8%)	30.1 (NA)	25.1 (18.3%)	23.4 (32.0%)	24.7 (15.5%)	-	-	-	27.0 (51.8%)	30.1 (NA)	25.1 (18.3%)	23.4 (32.0%)	24.7 (15.5%)
AUC _{0–last} , µg*day/mL	-	-	-	41.2 (12.2%)	157.6 (12.5%)	380.1 (18.6%)	1314.5 (22.4%)	3833.9 (10.8%)	-	-	-	41.2 (12.2%)	157.6 (12.5%)	380.1 (18.6%)	1314.5 (22.4%)	3833.9 (10.8%)
CL, mL/min	-	-	-	0.11 (27.9%)	0.08 (NA)	0.10 (2.2%)	0.09 (11.6%)	0.11 (21.4%)	-	-	-	0.11 (27.9%)	0.08 (NA)	0.10 (2.2%)	0.09 (11.6%)	0.11 (21.4%)
Third KY1005 dose																
T _{max} , h	-	-	-	4.5 (0.5–12.5)	4.5 (4.5–24.0)	4.5 (0.5–12.5)	24.0 (24.0–24.0)	0.5 (0.5–24.0)	-	-	-	4.5 (0.5–12.5)	4.5 (4.5–24.0)	4.5 (0.5–12.5)	24.0 (24.0–24.0)	0.5 (0.5–24.0)
C _{max} , µg/mL	-	-	-	3.0 (15.7%)	11.5 (16.6%)	28.8 (18.3%)	73.8 (9.9%)	249.6 (14.4%)	-	-	-	3.0 (15.7%)	11.5 (16.6%)	28.8 (18.3%)	73.8 (9.9%)	249.6 (14.4%)
t _{1/2} , days	-	-	-	27.7 (20.5%)	28.3 (24.6%)	43.1 (24.1%)	41.7 (25.9%)	24.3 (17.3%)	-	-	-	27.7 (20.5%)	28.3 (24.6%)	43.1 (24.1%)	41.7 (25.9%)	24.3 (17.3%)
AUC _{0–last} , µg*day/mL	-	-	-	53.0 (15.2%)	195.5 (9.9%)	551.9 (8.1%)	1674.8 (10.6%)	4505.2 (9.7%)	-	-	-	53.0 (15.2%)	195.5 (9.9%)	551.9 (8.1%)	1674.8 (10.6%)	4505.2 (9.7%)
CL, mL/min	-	-	-	0.09 (20.3%)	0.07 (21.0%)	0.06 (13.1%)	0.06 (22.9%)	0.10 (35.7%)	-	-	-	0.09 (20.3%)	0.07 (21.0%)	0.06 (13.1%)	0.06 (22.9%)	0.10 (35.7%)

Data displayed as mean (coefficient of variation %) and for T_{max} as median (range).

AUC_{0–last}, area under the curve from zero point to the last measurable concentration; CL, clearance; C_{max}, peak serum concentration; MAD, multiple ascending dose; NA, no regression line could be fitted; SAD, single ascending dose; t_{1/2}, half-life; T_{max}, time at which the C_{max} is observed.

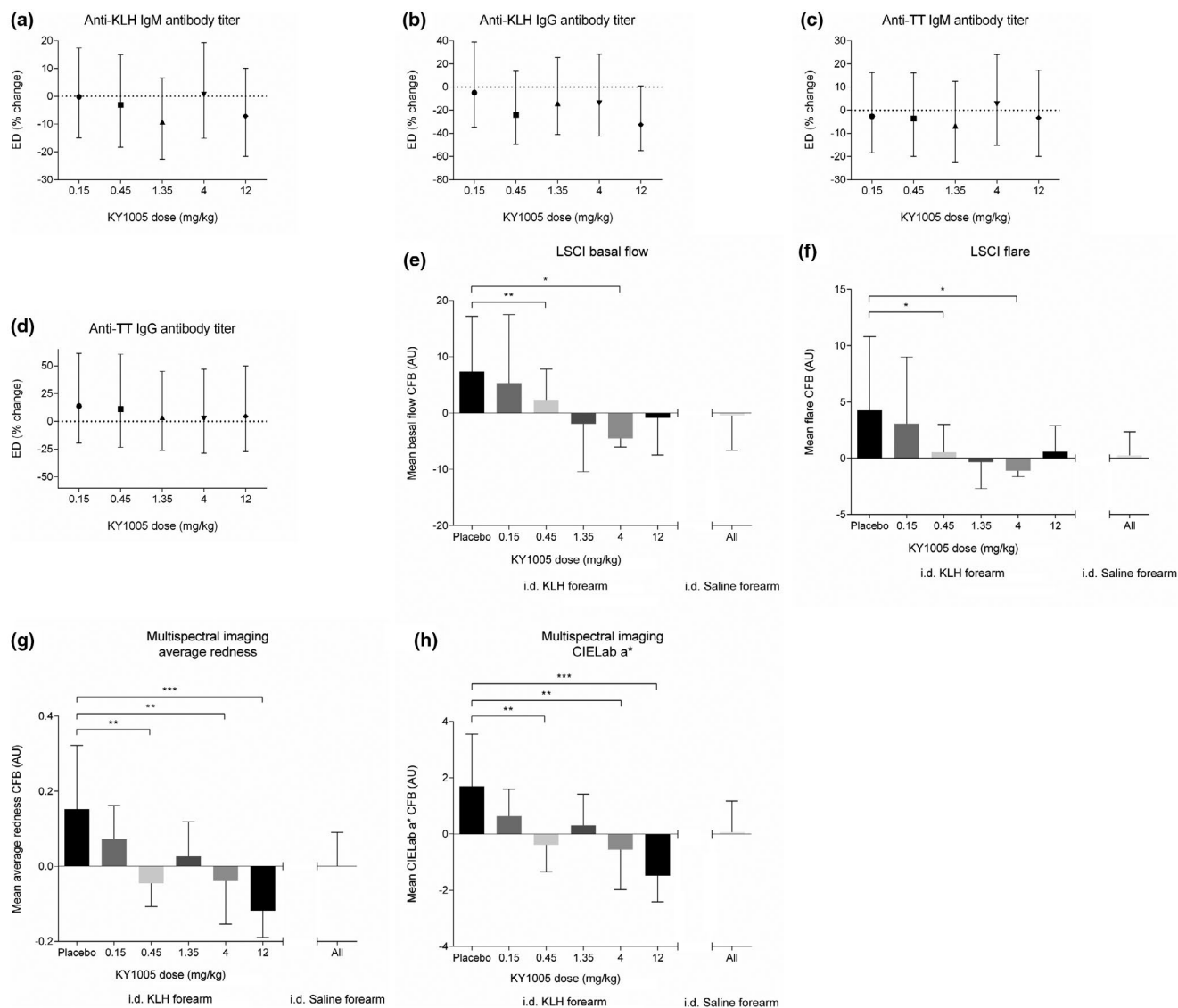


Figure 3 Anti-KLH IgM (a) and IgG antibody titers (b), anti-TT IgM (c), and IgG antibody titers (d) 21 days after KLH and TT immunizations, cutaneous blood perfusion by LSCI basal flow (e) and LSCI flare (f), erythema by multispectral imaging average redness (g), and multispectral imaging CIELab a* (h) 2 days after intradermal KLH administration by treatment group. Data are shown as estimated difference percentage change (95% confidence interval) for a to d and as mean CFB (SD) for e to h. AU, arbitrary unit; CFB, change from baseline; ED, estimated difference; i.d., intradermal; KLH, keyhole limpet hemocyanin; LSCI, laser speckle contrast imaging; TT, tetanus toxoid. The *P* values are based on estimated differences between groups with correction for baseline measurements and saline administration. **P* < 0.05, ***P* < 0.01, ****P* < 0.001.

was the first KY1005 exposure and the subject had never received an intravenous administration of any kind. A pseudoallergy might have been the cause of the AEs. This pseudoallergy was classified as grade 1, since no medication was administered and the symptoms resolved spontaneously within 2 hours. No other AE-related discontinuations of KY1005 treatment occurred. AEs observed after monoclonal antibody administration are usually related to infection and immunomodulation.³⁸ No increase in infection rate after KY1005 treatment was observed compared with placebo, possibly explained by the fact that the OX40-OX40L pathway is primarily involved in sustaining T cell activation and not in the initial stimulation.⁷

PK analyses displayed a nonlinear increase in mean serum concentrations of KY1005. The PK profile of KY1005 displayed nonlinear target-mediated drug disposition (TMDD)³⁹ as is commonly observed for monoclonal antibodies.⁴⁰ At low KY1005 concentrations, a high CL was observed as a large portion of the drug is likely cleared via drug-target binding and subsequent degradation of the drug-target complex. Saturation of TMDD presumably led to lower observed CL at higher KY1005 doses. The mean KY1005 $t_{1/2}$ of 24.3 days was similar to the expected predicted mean $t_{1/2}$ of 26 ± 7 days based on preclinical experiments. ADAs may influence the clearance of monoclonal antibodies. We did not find evidence for ADA-mediated

Table 3 Summary statistics for pharmacodynamic end points

Pharmacodynamic parameter	KY1005 dose level				
	0.15 mg/kg (N = 6)	0.45 mg/kg (N = 5)	1.35 mg/kg (N = 6)	4 mg/kg (N = 5)	12 mg/kg (N = 5)
Anti-KLH IgM (% change)	-0.1% (-14.9%–17.4%)	-3.1% (-18.3%–14.9%)	-9.2% (-22.7%–6.6%)	0.7% (-15.1%–19.4%)	-7.1% (-21.7%–10.1%)
Anti-KLH IgG (% change)	-4.8% (-34.8%–39.0%)	-23.9% (-49.0%–13.5%)	-13.9% (-41.0%–25.7%)	-14.0% (-42.4%–28.3%)	-32.4% (-54.7%–0.9%)
Anti-TT IgM (% change)	-2.6% (-18.4%–16.2%)	-3.6% (-20.0%–16.1%)	-6.7% (-22.6%–12.5%)	2.7% (-15.1%–24.1%)	-3.2% (-20.0%–17.2%)
Anti-TT IgG (% change)	13.8% (-19.6%–61.2%)	11.0% (-23.2%–60.5%)	3.6% (-26.1%–45.2%)	2.4% (-28.6%–46.9%)	4.6% (-27.0%–49.9%)
LSCI basal flow (AU)	-3.3 (-11.3–4.7)	-13.4 (-23.0–-3.8)**	-6.2 (-14.2–1.8)	-11.0 (-19.8–-2.3)*	-5.9 (-14.4–2.5)
LSCI flare (AU)	-2.2 (-6.9–2.4)	-7.5 (-13.2–-1.8)*	-4.5 (-9.0–0.1)	-5.8 (-10.8–-0.9)*	-3.1 (-7.9–1.8)
Multispectral imaging average redness (AU)	-0.04 (-0.16–0.09)	-0.20 (-0.32–-0.07)**	-0.11 (-0.23–0.01)	-0.17 (-0.29–-0.05)**	-0.23 (-0.35–-0.11)***
Multispectral imaging CIELab a* (AU)	-0.7 (-2.1–0.6)	-2.1 (-3.5–-0.8)**	-1.2 (-2.5–0.1)	-2.0 (-3.4–-0.7)**	-2.6 (-4.0–-1.3)***

Data displayed as estimated difference (95% confidence interval).

AU, arbitrary unit; KLH, keyhole limpet hemocyanin; LSCI, laser speckle contrast imaging; TT, tetanus toxoid.

* $P < 0.05$, ** $P < 0.01$, *** $P < 0.001$.

clearance of KY1005, which may reflect no such effect, or an insufficient number of subjects exposed. At approximate concentrations of > 2 mg/mL, KY1005 clearance remained relatively stable, which might indicate TMDD saturation and possibly 100% target binding.

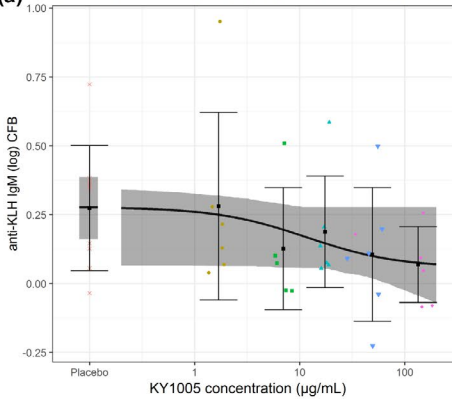
Between 25% and 50% of KY1005-treated participants had positive ADA responses, but this was not associated with unexpected changes in the serum PK indicating, where present, the ADAs were non or only weakly neutralizing. The number of subjects with ADAs increased with increasing KY1005 dose in SAD cohorts. In MAD cohorts, however, the largest number of subjects positive for ADAs was observed at the lowest dose regimen (0.15 mg/kg), with no subjects developing detectable ADAs at the highest dose regimen (12 mg/kg). This observation is in keeping with the pattern expected with increasing suppression of ADA development at higher doses reaching saturation of the target and suppression of antibody response to KY1005.

No statistically significant reduced antibody titers against KLH and TT were observed after KY1005 treatment compared with placebo. The lack of effect and consistency by dose group most possibly reflects the small sample size and normal variability observed with respect to the PD markers. Despite this the observed data indicated moderate pharmacological activity of KY1005 at loading doses of 0.45 mg/kg and above. Importantly, combined individual data of all KY1005 serum concentrations plotted against anti-KLH IgM and IgG antibody titers revealed a modest treatment effect of KY1005. This treatment effect was stronger on anti-KLH IgG compared with IgM possibly explained by the time window of 21 days between baseline and postimmunization measurements and class switching between the isotypes. Our results are translationally confirmed by a previously published study performed in mice, which showed that blockade of the OX40-OX40L

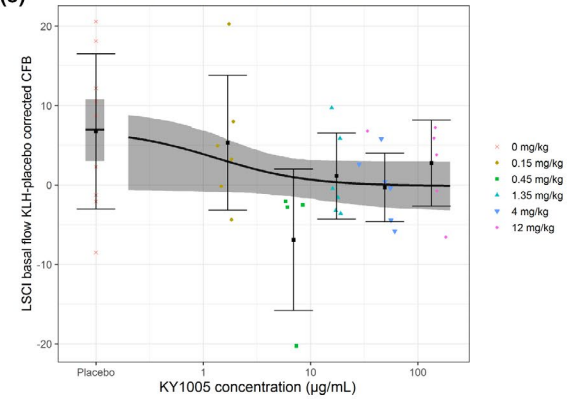
signaling pathway inhibited T cell-dependent antibody production after KLH immunization.⁴¹ Based on these results, inhibition of OX40L may possibly interfere with T cell-dependent antibody production. Furthermore, maximum effects of KY1005 on anti-KLH antibody titers seem to have been reached based on the concentration-effect models. The recall antigen response to TT is probably not sufficiently suppressed as memory B cells are able to differentiate to plasma cells in the absence of T cells⁴² and other pathways besides OX40-OX40L can still be stimulated. Although it is known that T cell-dependent B cell activation requires CD40-CD40L costimulatory factors following T cell receptor-Major Histocompatibility Complex II-peptide binding,^{43,44} the exact mechanism and pathways underlying T cell-dependent B cell activation and the role of OX40-OX40L signaling remain to be elucidated. *Ex vivo* antigen rechallenges of lymphocytes isolated from KY1005-exposed volunteers may provide additional insight and improved characterization of immune pathways modulated by OX40-OX40L inhibition.

The KLH skin challenge model used in the present study was previously validated in healthy volunteers using multispectral imaging and LSCI, similar to the methods used in the current study.³⁰ Various clinical studies have demonstrated that KLH is a potent immunostimulatory antigen, producing a robust immune response, and having an excellent safety profile.⁴⁵ Formally, the study was not powered for detection of KY1005 effects on the skin challenge response;³⁰ the sample size used is common in first-in-human trials and the KLH-based PD skin challenge end points were exploratory in nature only. Despite being underpowered, we found that KY1005 suppressed the skin challenge response following intradermal KLH administration as cutaneous blood perfusion and erythema were lower in KY1005-treated subjects compared with placebo. The half

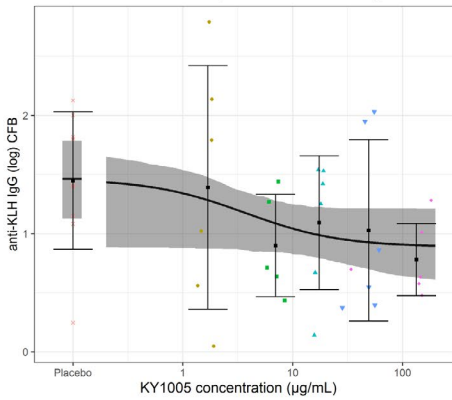
(a) Emax model of KY1005 exposure and anti-KLH IgM titres



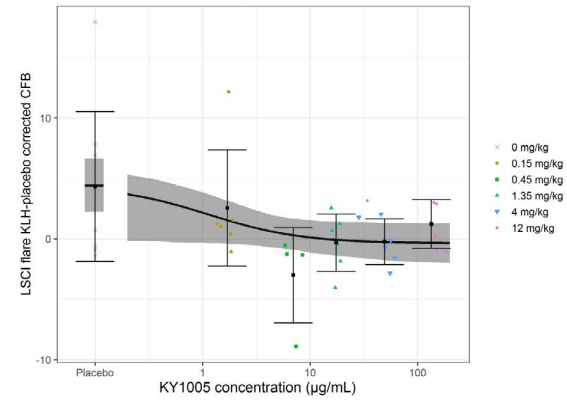
(e) Emax model of KY1005 exposure and LSCI basal flow



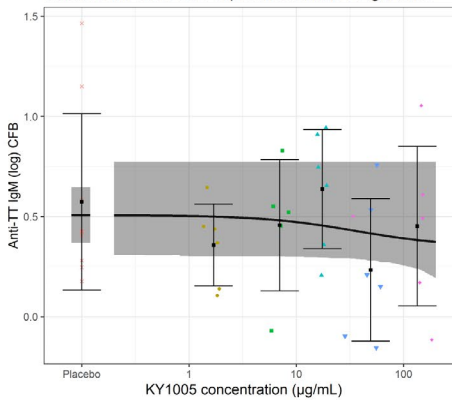
(b) Emax model of KY1005 exposure and anti-KLH IgG titres



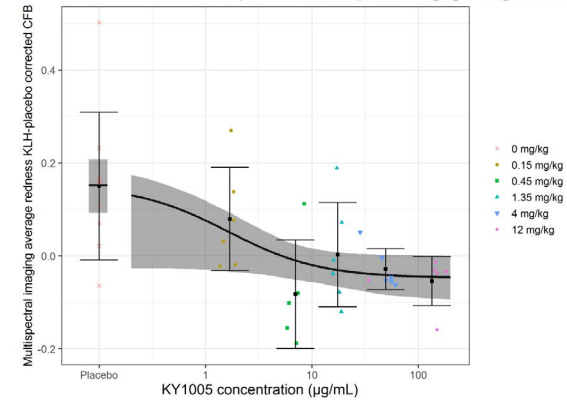
(f) Emax model of KY1005 exposure and LSCI flare



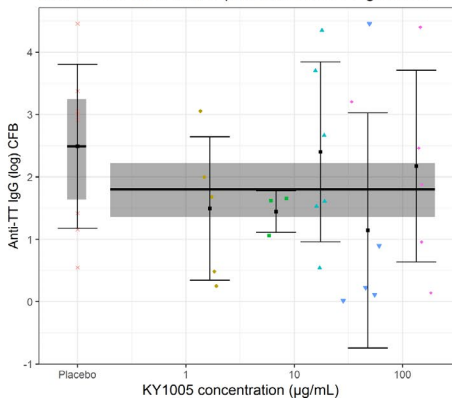
(c) Emax model of KY1005 exposure and anti-TT IgM titres



(g) Emax model of KY1005 exposure and multispectral imaging average redness



(d) Emax model of KY1005 exposure and anti-TT IgG titres



(h) Emax model of KY1005 exposure and multispectral imaging CIELab a*

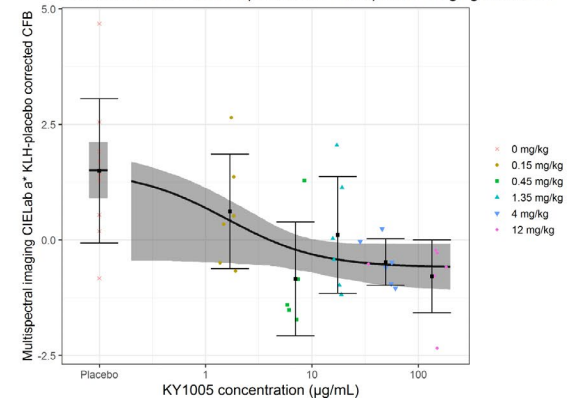


Figure 4 E_{\max} model of KY1005 exposure and anti-KLH IgM (a), anti-KLH IgG (b), anti-TT IgM (c), anti-TT IgG (d), LSCI basal flow (e), LSCI flare (f), multispectral imaging average redness (g), and multispectral imaging CIELab a* (h). Dots represent individual data points. Black squares (error bars) represent mean (SD) of observed data per dose level. Black line (grey area) represents model predicted mean (90% confidence interval). Data are shown as log₁₀ change from baseline ratios vs. KY1005 concentration. CFB, change from baseline; E_{\max} , maximum effect; KLH, keyhole limpet hemocyanin; LSCI, laser speckle contrast imaging; TT, tetanus toxoid.

maximal inhibitory concentration (IC_{50}) of KY1005 in preclinical *in vitro* experiments was $0.30 \text{ nM} \pm 0.01 \text{ nM}$ (mean \pm standard error of the mean). The KY1005 starting dose of 0.006 mg/kg corresponds to a concentration of 1.0 nM and was based on the MABEL principle using *in vitro* data obtained in human MLR experiments. Substantial decreases in cutaneous blood perfusion and erythema as a result of skin challenge response were initially observed at a KY1005 dose of 0.45 mg/kg , which corresponds to a concentration of 75 nM , a 250-fold higher dose compared to the IC_{50} . In contrast to KY1005's effects on anti-KLH antibodies, the effects on the skin challenge response were seen to be dose-dependent. Accordingly, exposure-response analyses displayed a treatment effect of KY1005 on all skin challenge endpoints (LSCI basal flow and flare and multispectral imaging average redness and CIELab a* values).

T cell-dependent immune responses are complex to monitor and to modulate. Therefore, a successful translation of the observed PD effects of KY1005 (suppression of the KLH-driven responses in healthy volunteers) to clinical effects in patients with immune-mediated diseases is challenging. However, the unremarkable safety and tolerability profile of KY1005 combined with the observed immunomodulatory properties support the potential of KY1005 as a novel compound targeting the OX40-OX40L signaling pathway for immune-mediated disorders. Based on the data generated in the present study, a successful phase IIa trial of KY1005 has recently been completed in patients with atopic dermatitis and a phase IIb trial is planned.

SUPPORTING INFORMATION

Supplementary information accompanies this paper on the *Clinical Pharmacology & Therapeutics* website (www.cpt-journal.com).

FUNDING

Kymab Ltd. (Cambridge, UK) was the sponsor for the study and funded all study related activities.

CONFLICT OF INTEREST

J.P., S.G., M.Y., B.P.B., N.B., S.Q., and R.W. are employed by the sponsor. All other authors declared no competing interests for this work.

AUTHOR CONTRIBUTIONS

All authors wrote the manuscript. J.P., B.P.B., M.Y., N.B., R.R., M.M., P.G., and M.S. designed the research. S.G., R.R., P.G., and M.S. performed the research. H.W., K.B., E.K., and D.Z. analyzed the data.

© 2022 The Authors. *Clinical Pharmacology & Therapeutics* published by Wiley Periodicals LLC on behalf of American Society for Clinical Pharmacology and Therapeutics

This is an open access article under the terms of the Creative Commons Attribution-NonCommercial License, which permits use, distribution and reproduction in any medium, provided the original work is properly cited and is not used for commercial purposes.

REFERENCES

- Munks, M.W., Mourich, D.V., Mittler, R.S., Weinberg, A.D. & Hill, A.B. 4–1BB and OX40 stimulation enhance CD8 and CD4 T-cell responses to a DNA prime, poxvirus boost vaccine. *Immunology* **112**, 559–566 (2004).
- Zaini, J. et al. OX40 ligand expressed by DCs costimulates NKT and CD4+ Th cell antitumor immunity in mice. *J. Clin. Investig.* **117**, 3330–3338 (2007).
- Melero, I., Hirschhorn-Cymerman, D., Morales-Kastresana, A., Sanmamed, M.F. & Wolchok, J.D. Agonist antibodies to TNFR molecules that costimulate T and NK cells. *Clin. Cancer Res.* **19**, 1044–1053 (2013).
- Baumann, R., Yousefi, S., Simon, D., Russmann, S., Mueller, C. & Simon, H.-U. Functional expression of CD134 by neutrophils. *Eur. J. Immunol.* **34**, 2268–2275 (2004).
- Gramaglia, I., Jember, A., Pippig, S.D., Weinberg, A.D., Killeen, N. & Croft, M. The OX40 costimulatory receptor determines the development of CD4 memory by regulating primary clonal expansion. *J. Immunol.* **165**, 3043–3050 (2000).
- Maxwell, J.R., Weinberg, A., Prell, R.A. & Vella, A.T. Danger and OX40 receptor signaling synergize to enhance memory T cell survival by inhibiting peripheral deletion. *J. Immunol.* **164**, 107–112 (2000).
- Mestas, J., Crampton, S.P., Hori, T. & Hughes, C.C.W. Endothelial cell co-stimulation through OX40 augments and prolongs T cell cytokine synthesis by stabilization of cytokine mRNA. *Int. Immunol.* **17**, 737–747 (2005).
- Linton, P.-J. et al. Costimulation via OX40L expressed by B cells is sufficient to determine the extent of primary CD4 cell expansion and Th2 cytokine secretion in vivo. *J. Exp. Med.* **197**, 875–883 (2003).
- Jenkins, S.J., Perona-Wright, G., Worsley, A.G.F., Ishii, N. & MacDonald, A.S. Dendritic cell expression of OX40 ligand acts as a costimulatory, not polarizing, signal for optimal Th2 priming and memory induction in vivo. *J. Immunol.* **179**, 3515–3523 (2007).
- Karulf, M., Kelly, A., Weinberg, A.D. & Gold, J.A. OX40 ligand regulates inflammation and mortality in the innate immune response to sepsis. *J. Immunol.* **185**, 4856–4862 (2010).
- Imura, A. et al. The human OX40/gp34 system directly mediates adhesion of activated T cells to vascular endothelial cells. *J. Exp. Med.* **183**, 2185–2195 (1996).
- Krimmer, D.I. et al. CD40 and OX40 ligand are differentially regulated on asthmatic airway smooth muscle. *Allergy* **64**, 1074–1082 (2009).
- Nakae, S. et al. Mast cells enhance T cell activation: importance of mast cell costimulatory molecules and secreted TNF. *J. Immunol.* **176**, 2238–2248 (2006).
- Kashiwakura, J.-I., Yokoi, H., Saito, H. & Okayama, Y. T Cell proliferation by direct cross-talk between OX40 ligand on human mast cells and OX40 on human T cells: comparison of gene expression profiles between human tonsillar and lung-cultured mast cells. *J. Immunol.* **173**, 5247–5257 (2004).
- Takeda, I. et al. Distinct roles for the OX40-OX40 ligand interaction in regulatory and nonregulatory T cells. *J. Immunol.* **172**, 3580–3589 (2004).
- Webb, G.J., Hirschfield, G.M. & Lane, P.J.L. OX40, OX40L and autoimmunity: a comprehensive review. *Clin. Rev. Allergy Immunol.* **50**, 312–332 (2016).
- Gaspal, F.M. et al. Abrogation of CD30 and OX40 signals prevents autoimmune disease in FoxP3-deficient mice. *J. Exp. Med.* **208**, 1579–1584 (2011).
- Gwyer Findlay, E. et al. OX40L blockade is therapeutic in arthritis, despite promoting osteoclastogenesis. *Proc. Natl. Acad. Sci. USA* **111**, 2289–2294 (2014).

19. Murata, K., Nose, M., Ndhlovu, L.C., Sato, T., Sugamura, K. & Ishii, N. Constitutive OX40/OX40 ligand interaction induces autoimmune-like diseases. *J. Immunol.* **169**, 4628–4636 (2002).
20. Guttman-Yassky, E. *et al.* GBR 830, an anti-OX40, improves skin gene signatures and clinical scores in patients with atopic dermatitis. *J. Allergy Clin. Immunol.* **144**, 482–493 (2019).
21. Papp, K.A., Gooderham, M.J., Girard, G., Raman, M. & Strout, V. Phase I randomized study of KHK4083, an anti-OX40 monoclonal antibody, in patients with mild to moderate plaque psoriasis. *J. Eur. Acad. Dermatol. Venereol.* **31**, 1324–1332 (2017).
22. Pakala, S.V., Bansal-Pakala, P., Halteman, B.S. & Croft, M. Prevention of diabetes in NOD mice at a late stage by targeting OX40/OX40 ligand interactions. *Eur. J. Immunol.* **34**, 3039–3046 (2004).
23. Totsuka, T. *et al.* Therapeutic effect of anti-OX40L and anti-TNF- α MAbs in a murine model of chronic colitis. *Am. J. Physiol. Gastrointest. Liver Physiol.* **284**, G595–G603 (2003).
24. Yoshioka, T. *et al.* Contribution of OX40/OX40 ligand interaction to the pathogenesis of rheumatoid arthritis. *Eur. J. Immunol.* **30**, 2815–2823 (2000).
25. Zhang, Z. *et al.* Activation of OX40 augments Th17 cytokine expression and antigen-specific uveitis. *Am. J. Pathol.* **177**, 2912–2920 (2010).
26. Nohara, C. *et al.* Amelioration of experimental autoimmune encephalomyelitis with anti-OX40 ligand monoclonal antibody: a critical role for OX40 ligand in migration, but not development, of pathogenic T cells. *J. Immunol.* **166**, 2108–2115 (2001).
27. Elyaman, W. *et al.* Distinct functions of autoreactive memory and effector CD4⁺ T cells in experimental autoimmune encephalomyelitis. *Am. J. Pathol.* **173**, 411–422 (2008).
28. Gauvreau, G.M. *et al.* OX 40L blockade and allergen-induced airway responses in subjects with mild asthma. *Clin. Exp. Allergy* **44**, 29–37 (2014).
29. Tkachev, V. *et al.* Combined OX40L and mTOR blockade controls effector T cell activation while preserving T reg reconstitution after transplant. *Sci. Transl. Med.* **9**, eaan3085 (2017).
30. Saghari, M. *et al.* A randomized controlled trial with a delayed-type hypersensitivity model using keyhole limpet haemocyanin to evaluate adaptive immune responses in man. *Br. J. Clin. Pharmacol.* **87**, 1953–1962 (2021).
31. Boulton, C., Meiser, K., David, O.J. & Schmouder, R. Pharmacodynamic effects of steady-state fingolimod on antibody response in healthy volunteers: a 4-week, randomized, placebo-controlled, parallel-group, multiple-dose study. *J. Clin. Pharmacol.* **52**, 1879–1890 (2012).
32. Ferbas, J. *et al.* A novel assay to measure B cell responses to keyhole limpet haemocyanin vaccination in healthy volunteers and subjects with systemic lupus erythematosus. *Br. J. Clin. Pharmacol.* **76**, 188–202 (2013).
33. Smith, A., Vollmer-Conna, U., Bennett, B., Wakefield, D., Hickie, I. & Lloyd, A. The relationship between distress and the development of a primary immune response to a novel antigen. *Brain Behav. Immun.* **18**, 65–75 (2004).
34. Smith, A.J., Vollmer-Conna, U., Bennett, B., Hickie, I.B. & Lloyd, A.R. Influences of distress and alcohol consumption on the development of a delayed-type hypersensitivity skin test response. *Psychosom. Med.* **66**, 614–619 (2004).
35. Smith, T.P., Kennedy, S.L. & Fleshner, M. Influence of age and physical activity on the primary in vivo antibody and T cell-mediated responses in men. *J. Appl. Physiol.* **97**, 491–498 (2004).
36. Boelens, P.G. *et al.* Primary immune response to keyhole limpet haemocyanin following trauma in relation to low plasma glutamine. *Clin. Exp. Immunol.* **136**, 356–364 (2004).
37. Ly, B.C.K., Dyer, E.B., Feig, J.L., Chien, A.L. & Del Bino, S. Research techniques made simple: cutaneous colorimetry: a reliable technique for objective skin color measurement. *J. Invest. Dermatol.* **140**, 3–12 (2020).
38. Giezen, T.J., Mantel-Teeuwisse, A.K., Straus Sabine, M.J.M., Schellekens, H., Leufkens, H.G.M. & Egberts, A.C.G. Safety-related regulatory actions for biologicals approved in the United States and the European Union. *JAMA* **300**, 1887 (2008).
39. Mager, D.E. Target-mediated drug disposition and dynamics. *Biochem. Pharmacol.* **72**, 1–10 (2006).
40. Liu, L. Pharmacokinetics of monoclonal antibodies and Fc-fusion proteins. *Protein Cell* **9**, 15–32 (2018).
41. Stüber, E. & Strober, W. The T cell-B cell interaction via OX40-OX40L is necessary for the T cell-dependent humoral immune response. *J. Exp. Med.* **183**, 979–989 (1996).
42. Kurosaki, T., Kometani, K. & Ise, W. Memory B cells. *Nat. Rev. Immunol.* **15**, 149–159 (2015).
43. Blum, J.S., Wearsch, P.A. & Cresswell, P. Pathways of antigen processing. *Annu. Rev. Immunol.* **31**, 443–473 (2013).
44. Crotty, S. A brief history of T cell help to B cells. *Nat. Rev. Immunol.* **15**, 185–189 (2015).
45. Swaminathan, A., Lucas, R.M., Dear, K. & McMichael, A.J. Keyhole limpet haemocyanin - a model antigen for human immunotoxicological studies. *Br. J. Clin. Pharmacol.* **78**, 1135–1142 (2014).